Highlights

A thermodynamically consistent formulation of the Johnson-Cook model

Charles Mareau

- The model of Johnson and Cook is revisited from the view point of thermodynamics
- The resulting analysis shows that the original model displays some limitations
- Such limitations are circumvented with an alternative but nevertheless similar model
- Some applications of both the original and alternative models are presented

A thermodynamically consistent formulation of the Johnson-Cook model

Charles Mareau

Arts et Métiers Paris Tech - LAMPA

Arts et Métiers ParisTech, Campus d'Angers, LAMPA, 2 bd du Ronceray, 49035 Angers Cedex 1, France

Abstract

The model of Johnson and Cook, which includes a viscoplastic flow rule and a damage criterion, is widely used to describe the mechanical behaviour of metallic materials subjected to severe loading conditions, such as those encountered during fabrication operations or impact. This model has been built on empirical, rather than physical, grounds. The present paper therefore aims at revisiting the model of Johnson and Cook from the view point of thermodynamics with internal variables. The interest of this approach is twofold. First, it provides a guide for the construction of a complete thermomechanical constitutive model, with some constitutive relations not only for the stress tensor but also specific internal energy, specific entropy and heat flux vector. Second, it allows highlighting some possible limitations of the original model of Johnson and Cook. Such limitations can be circumvented with an alternative model, which is described in the present work. For illustration purpose, some applications of both the original and alternative models are presented in the final section.

Keywords: Johnson-Cook, Viscoplasticity, Damage, Thermodynamics, Finite strain

1. Introduction

During fabrication operations or impacts, materials often experience a wide range of strain rates and temperatures. Different models have therefore been developed to include the impact of strain rate and temperature on the mechanical behaviour of solid materials. Relying on either empirical or

physical arguments, these models provide some relations to (i) connect the flow stress to the equivalent plastic strain, the equivalent plastic strain rate and the temperature and (ii) determine whether the conditions for fracture are met or not. The former set of relations is usually referred to as the flow rule while the latter is a fracture criterion.

The most common model for metallic materials is likely the one of Johnson and Cook (1983, 1985), which includes a thermo-viscoplastic flow rule and a ductile damage criterion. This model is largely used for the numerical simulation of fabrication operations, with numerous applications to machining (Umbrello et al., 2007; Shrot and Bäker, 2012; Hor et al., 2013; Agmell et al., 2014) as well as forging (Yoo and Yang, 1997; Djavanroodi et al., 2019). It has been built upon an experimental basis, with some observations of both the deformation behaviour and fracture behaviour of different metallic materials over a wide range of strain rates and temperatures. The resulting flow rule is based on a multiplicative decomposition of the flow stress into strain hardening, strain-rate hardening and thermal softening contributions. To extend the range of applicability of the Johnson-Cook model, some modified versions of this model have emerged. For instance, many options have been explored to consider the coupled effects of temperature and strain rate (He et al., 2013; Chen et al., 2010; Wang et al., 2017). A modified version has also been proposed by Couque et al. (2006) to account for the dislocation drag regime that governs the deformation behaviour at very high strain rates ($\geq 10^5$ s^{-1}). Camacho and Ortiz (1997) modified the strain-rate sensitivity term of the viscoplastic flow rule to describe the behaviour at low strain rates. A strain-rate softening contribution, which is ignored in the original model, has been included in the model developed by Zhao et al. (2017).

Though the model of Johnson and Cook (1983, 1985) is often used for thermomechanical simulations, it has not been developed in a consistent thermodynamic framework. The Johnson-Cook model therefore has two major drawbacks. First, it does not provide any constitutive relation for thermodynamic quantities such as internal energy, heat flux vector or entropy. The direct consequence is that it is not possible to identity the expressions of the different heat sources contributing to the heat diffusion equation. Second, the compatibility of constitutive relations with the fundamental laws of thermodynamics cannot be checked so that violations of these laws cannot be excluded. Specifically, the non-negativity of the heat dissipation source, which is implied by the second of law of thermodynamics, is not ensured.

The present work therefore aims at reformulating the Johnson-Cook model

in a consistent thermodynamic framework. For this purpose, the concept of internal state variables (Maugin and Muschik, 1994) is used to consider the microstructural transformations (e.g. strain hardening, ductile damage) that have been included in the original Johnson-Cook model. This concept provides a way of revisiting the Johnson-Cook model with an alternative point of view. This allows deriving a complete thermomechanical finite strain constitutive model, with some constitutive relations not only for the stress tensor but also specific internal energy, specific entropy and heat flux vector. The present paper is organized as follows. The first section is dedicated to the description of constitutive relations. Because the original Johnson-Cook model displays some limitations, different options for considering thermal softening and strain rate effects are explored. For illustration purpose, some applications, which allow comparing these options, are presented in the second section.

2. Constitutive relations

For the purpose of describing the evolution of a deformable body, the mass, momentum and energy conservation equations must be supplemented with a constitutive model. Within a thermomechanical context, a constitutive model consists of some relations for the stress state, the specific entropy, the specific internal energy and the heat flux vector. Some additional evolution relations can also be included to consider the microstructural transformations (e.g. hardening, damage) having an impact on the thermomechanical behaviour of a material point. In the present section, a set of constitutive relations, which includes the Johnson-Cook viscoplastic flow rule and the Johnson-Cook fracture criterion, is detailed.

2.1. Kinematics

For the presentation of the constitutive model, a single material point is considered. For such a material point, the multiplicative decomposition of the deformation gradient tensor $\boldsymbol{F}$ suggested by Lee (1969) is adopted so that:

$$\boldsymbol{F} = \boldsymbol{F}_\theta \cdot \boldsymbol{F}_p \tag{1}$$

where $\boldsymbol{F}_\theta$ and $\boldsymbol{F}_p$ are respectively the thermoelastic and plastic contributions to the deformation gradient tensor. The concept of the isoclinic relaxed intermediate configuration proposed by Mandel (1973) is used here as it provides a convenient way of formulating constitutive models.

Because we restrict our attention to the specific, but rather common, case where the plastic flow is incompressible, the initial and current mass densities ρ_0 and ρ are connected to each other with:

$$\rho_0 = J\rho \tag{2}$$

with $J = \det\boldsymbol{F} = \det\boldsymbol{F}_\theta$.

In the following, the Green-Lagrange strain tensor $\boldsymbol{E}$ is used as a strain measure. According to the above multiplicative decomposition, the Green-Lagrange strain tensor $\boldsymbol{E}$ is separated into thermoelastic and plastic contributions as follows:

$$\boldsymbol{E} = \frac{1}{2}\left(\boldsymbol{F}^T \cdot \boldsymbol{F} - \mathbf{1}\right) = \boldsymbol{F}_p^T \cdot \tilde{\boldsymbol{E}}_\theta \cdot \boldsymbol{F}_p + \boldsymbol{E}_p \tag{3}$$

with:

$$\tilde{\boldsymbol{E}}_\theta = \frac{1}{2}\left(\boldsymbol{F}_\theta^T \cdot \boldsymbol{F}_\theta - \mathbf{1}\right) \tag{4}$$

$$\boldsymbol{E}_p = \frac{1}{2}\left(\boldsymbol{F}_p^T \cdot \boldsymbol{F}_p - \mathbf{1}\right) \tag{5}$$

While $\boldsymbol{E}$ and $\boldsymbol{E}_p$ are associated with the initial configuration, the thermoelastic strain tensor $\tilde{\boldsymbol{E}}_\theta$ is attached to the isoclinic intermediate configuration.

In a similar fashion, the velocity gradient tensor $\boldsymbol{L}$ is decomposed according to:

$$\boldsymbol{L} = \dot{\boldsymbol{F}} \cdot \boldsymbol{F}^{-1} = \boldsymbol{L}_\theta + \boldsymbol{F}_\theta \cdot \tilde{\boldsymbol{L}}_p \cdot \boldsymbol{F}_\theta^{-1} \tag{6}$$

with:

$$\boldsymbol{L}_\theta = \dot{\boldsymbol{F}}_\theta \cdot \boldsymbol{F}_\theta^{-1} \tag{7}$$

$$\tilde{\boldsymbol{L}}_p = \dot{\boldsymbol{F}}_p \cdot \boldsymbol{F}_p^{-1} \tag{8}$$

The above relation indicates that $\tilde{\boldsymbol{L}}_p$ is associated with the intermediate configuration while both $\boldsymbol{L}$ and $\boldsymbol{L}_\theta$ are attached to the current configuration.

2.2. Thermodynamics

For a closed system, according to the first law of thermodynamics (i.e. energy conservation), the evolution of the specific internal energy u for a material point is given by:

$$\dot{u} = \frac{\boldsymbol{\sigma} : \boldsymbol{L}}{\rho} - \frac{\boldsymbol{\nabla} \cdot \boldsymbol{q}}{\rho} + r \tag{9}$$

where $\boldsymbol{\sigma}$ is the Cauchy stress tensor, $\boldsymbol{q}$ is the heat flux density vector and r is the specific heat source. From the decomposition of the velocity gradient tensor $\boldsymbol{L}$, the above energy conservation equation is conveniently reformulated on the intermediate configuration as follows:

$$\dot{u} = \frac{\tilde{\boldsymbol{S}} : \dot{\tilde{\boldsymbol{E}}}_\theta}{\rho_0} + \frac{\tilde{\boldsymbol{\Sigma}} : \tilde{\boldsymbol{L}}_p}{\rho_0} - \frac{\tilde{\boldsymbol{\nabla}} \cdot \tilde{\boldsymbol{Q}}}{\rho_0} + r \tag{10}$$

where $\tilde{\boldsymbol{S}}$ is second Piola-Kirchoff stress tensor associated with the intermediate configuration and $\tilde{\boldsymbol{\Sigma}}$ is the Mandel stress tensor (Mandel, 1973). These stress measures are connected to the Cauchy stress tensor $\boldsymbol{\sigma}$ with:

$$\tilde{\boldsymbol{S}} = J\boldsymbol{F}_\theta^{-1} \cdot \boldsymbol{\sigma} \cdot \boldsymbol{F}_\theta^{-T} \tag{11}$$

$$\tilde{\boldsymbol{\Sigma}} = J\boldsymbol{F}_\theta^{T} \cdot \boldsymbol{\sigma} \cdot \boldsymbol{F}_\theta^{-T} \tag{12}$$

The heat flux density vector $\tilde{\boldsymbol{Q}}$ and the $\tilde{\boldsymbol{\nabla}}$ operator, which appear in equation (10), are defined according to:

$$\tilde{\boldsymbol{Q}} = J\boldsymbol{F}_\theta^{-1} \cdot \boldsymbol{q} \tag{13}$$

$$\tilde{\boldsymbol{\nabla}} = \boldsymbol{\nabla} \cdot \boldsymbol{F}_\theta \tag{14}$$

According to the second law of thermodynamics, the rate of entropy production per unit mass η must be non-negative. For a closed system, the corresponding inequality is:

$$\eta = \dot{s} - \frac{r}{T} + \frac{1}{\rho}\boldsymbol{\nabla} \cdot \left(\frac{\boldsymbol{q}}{T}\right) \geq 0 \tag{15}$$

where s is the specific entropy and T is the absolute temperature. The expression of the specific dissipation source d is obtained from:

$$d = \eta T \geq 0 \tag{16}$$

$$= \dot{s}T - r + \frac{1}{\rho}\boldsymbol{\nabla} \cdot \boldsymbol{q} - \frac{1}{\rho T}\boldsymbol{q} \cdot \boldsymbol{\nabla} T \geq 0 \tag{17}$$

Using the local form (9) of the first law of thermodynamics, one obtains the following expression of the specific dissipation source d:

$$d = \frac{\boldsymbol{\sigma} : \boldsymbol{L}}{\rho} - \dot{u} + \dot{s}T - \frac{1}{\rho T}\boldsymbol{q} \cdot \boldsymbol{\nabla} T \geq 0 \tag{18}$$

The above dissipation inequality can alternatively be formulated on the intermediate configuration with (10), that is:

$$d = \frac{\tilde{\boldsymbol{S}} : \dot{\tilde{\boldsymbol{E}}}_\theta}{\rho_0} + \frac{\tilde{\boldsymbol{\Sigma}} : \tilde{\boldsymbol{L}}_p}{\rho_0} - \dot{u} + \dot{s}T - \frac{1}{\rho_0 T}\tilde{\boldsymbol{Q}} \cdot \tilde{\boldsymbol{\nabla}} T \geq 0 \tag{19}$$

2.3. Specific free energy

The specific Helmholtz free energy $a = u - sT$ is a thermodynamic potential that can be used to obtain the different state equations. In the following, the list of state variables, on which the specific free energy a depends, includes the thermoelastic strain tensor $\tilde{\boldsymbol{E}}_\theta$, the absolute temperature T, a scalar isotropic hardening variable P, which is the accumulated plastic strain, a tensorial kinematic hardening variable $\tilde{\boldsymbol{A}}_k$, which is a Green-Lagrange strain-like variable, and a damage variable D (with $D \in [0, 1]$). In the present work, the following decomposition of the specific free energy is assumed:

$$a\left[\tilde{\boldsymbol{E}}_\theta, \tilde{\boldsymbol{A}}_k, P, D, T\right] = a_\theta\left[\tilde{\boldsymbol{E}}_\theta, D, T\right] + a_{th}\left[T\right] + a_k\left[\tilde{\boldsymbol{A}}_k, D, T\right] + a_i\left[P, T\right] \tag{20}$$

The thermoelastic contribution a_θ is such that:

$$\begin{aligned} a_\theta = {} & \frac{1}{2\rho_0}\tilde{\boldsymbol{E}}_\theta : \mathbb{L} : \tilde{\boldsymbol{E}}_\theta - \frac{1}{\rho_0}\tilde{\boldsymbol{E}}_\theta : \mathbb{L} : \boldsymbol{\alpha}\left(T - T_0\right) \\ & + \frac{1}{2\rho_0}\boldsymbol{\alpha} : \left(\mathbb{L} - \mathbb{L}_u\right) : \boldsymbol{\alpha}\left(T - T_0\right)^2 \end{aligned} \tag{21}$$

The above expression uses the current and initial fourth-rank stiffness tensors $\mathbb{L}$ and $\mathbb{L}_u$, the second-rank thermal expansion tensor $\boldsymbol{\alpha}$ and the reference temperature T_0. The current fourth-rank stiffness tensor $\mathbb{L}$ depends on the damage variable D, the thermoelastic strain tensor $\tilde{\boldsymbol{E}}_\theta$ and the absolute temperature T. To consider the stiffness reduction associated with the development of damage, the following strategy is adopted. To account for possible closure effects, two different situations, which depend on the elastic strain tensor $\tilde{\boldsymbol{E}}_e = \tilde{\boldsymbol{E}}_\theta - \boldsymbol{\alpha}\left(T - T_0\right)$, are considered:

$$\mathbb{L} = \begin{cases} \mathbb{L}_t, & \tilde{\boldsymbol{E}}_e : \mathbf{1} \geq 0 \\ \mathbb{L}_c, & \tilde{\boldsymbol{E}}_e : \mathbf{1} < 0 \end{cases} \tag{22}$$

In the above equation, $\mathbb{L}_t$ (respectively $\mathbb{L}_c$) is the stiffness tensor corresponding to a positive (respectively negative) spherical elastic strain tensor. At a

given time t, the stiffness tensors $\mathbb{L}_t$ and $\mathbb{L}_c$ are calculated from the damage variable D and the initial stiffness tensor $\mathbb{L}_u$ with:

$$\mathbb{L}_t = (1 - D)\,\mathbb{L}_u \tag{23}$$

$$\mathbb{L}_c = \mathbb{L}_t + \mathbb{P}_s : (\mathbb{L}_u - \mathbb{L}_t) : \mathbb{P}_s \tag{24}$$

Equation (24) uses the fourth-rank spherical projection tensor $\mathbb{P}_s$. This tensor is defined by:

$$\mathbb{P}_s = \frac{1}{3}\mathbf{1} \otimes \mathbf{1} \tag{25}$$

According to equation (24), the stiffness tensor $\mathbb{L}_c$ is quite similar to $\mathbb{L}_t$, except that the spherical contribution is recovered because of closure effects. The impact of temperature on the undamaged stiffness tensor $\mathbb{L}_u$, which corresponds to the situation where $D = 0$, is described with:

$$\mathbb{L}_u = \mathbb{L}_0\,(1 - \beta\,(T - T_0)) \tag{26}$$

where $\mathbb{L}_0$ is the initial stiffness tensor at $T = T_0$ and β is a material parameter. To consider the evolution of thermal expansion properties with respect to temperature, the following relation is used:

$$\boldsymbol{\alpha} = \boldsymbol{\alpha}_0\,(1 + \zeta\,(T - T_0)) \tag{27}$$

where $\boldsymbol{\alpha}_0$ is the thermal expansion tensor at $T = T_0$ and ζ is a constant that allows considering the impact of temperature on thermal expansion properties.

The thermal contribution to free energy a_{th}, which solely depends on the absolute temperature T, is:

$$a_{th} = (c_0 - \gamma T_0)\left(T - T_0 - T\ln\left(\frac{T}{T_0}\right)\right) - \frac{1}{2}\gamma\,(T - T_0)^2 \tag{28}$$

As we shall see later, the evolution of the specific heat capacity as a function of temperature is controlled with the material parameters c_0 and γ.

The contribution of isotropic hardening to free energy is given by:

$$a_i = \frac{1}{\rho_0}\frac{B}{n+1}P^{n+1} \tag{29}$$

In the above equation, n is the strain hardening exponent and B is the temperature-dependent isotropic hardening modulus. To consider the yield

stress reduction caused by a temperature increase, the hardening modulus B must depend on the absolute temperature T. In the following, two different options are explored for the consideration of thermal softening:

$$B = B_0 \left(1 - \left(\frac{T - T_0}{T_M - T_0}\right)^m\right) \tag{30a}$$

$$B = B_0 \left(1 - \frac{T^m - T_0^m}{T_M^m - T_0^m}\right) \tag{30b}$$

where B_0 and m are material parameters and T_M is the absolute melting temperature. The first option (30a) corresponds to the original proposition of Johnson and Cook (1983). Except from the specific case where $m = 1$, this option has two major drawbacks. First, it is valid only for temperatures comprised between T_0 and T_M. Second, as will be discussed later, this option does not allow determining the specific heat capacity at $T = T_0$ when $m < 2$. The aforementioned drawbacks are avoided with the second option (30b), which is nevertheless similar to the original proposition of Johnson and Cook (1983) in the sense that the conditions $B[T_0] = B_0$ and $B[T_M] = 0$ are both met.

A quadratic form is assumed for the contribution a_k of the kinematic hardening variable $\tilde{\boldsymbol{A}}_k$ to free energy so that:

$$a_k = \frac{1}{2\rho_0} \tilde{\boldsymbol{A}}_k : \mathbb{K} : \tilde{\boldsymbol{A}}_k \tag{31}$$

where $\mathbb{K}$ is the kinematic hardening moduli tensor. The kinematic hardening moduli tensor is related to the damage variable in a manner similar to that used for the stiffness tensor. Depending on the spherical part of the kinematic hardening variable $\tilde{\boldsymbol{A}}_k$, the following situations are therefore considered:

$$\mathbb{K} = \begin{cases} \mathbb{K}_t, & \tilde{\boldsymbol{A}}_k : \mathbf{1} \geq 0 \\ \mathbb{K}_c, & \tilde{\boldsymbol{A}}_k : \mathbf{1} < 0 \end{cases} \tag{32}$$

The kinematic hardening moduli tensors $\mathbb{K}_t$ and $\mathbb{K}_c$ are given by:

$$\mathbb{K}_t = (1 - D)\, \mathbb{K}_u \tag{33}$$

$$\mathbb{K}_c = \mathbb{K}_t + \mathbb{P}_s : (\mathbb{K}_u - \mathbb{K}_t) : \mathbb{P}_s \tag{34}$$

The initial kinematic hardening moduli tensor $\mathbb{K}_u$ depends on the absolute temperature T according to:

$$\mathbb{K}_u = \mathbb{K}_0 \left(1 - \beta \left(T - T_0\right)\right) \tag{35}$$

The kinematic hardening moduli tensor $\mathbb{K}_0$ should be defined in agreement with the possible constraints due to material symmetry.

2.4. State equations

The specific free energy a allows determining the state equations connecting the state variables to the corresponding thermodynamic forces. First, with the above definition of the free energy, the second Piola-Kirchoff stress tensor $\tilde{\boldsymbol{S}}$ associated with the intermediate configuration is:

$$\tilde{\boldsymbol{S}} = \rho_0 \frac{\partial a}{\partial \tilde{\boldsymbol{E}}_\theta} \tag{36}$$

$$= \mathbb{L} : \left(\tilde{\boldsymbol{E}}_\theta - \boldsymbol{\alpha} \left(T - T_0 \right) \right) = \mathbb{L} : \tilde{\boldsymbol{E}}_e \tag{37}$$

The dual variable of the accumulated plastic strain P is the scalar stress R, which represents the yield stress increase associated with strain hardening. The stress R is connected to the accumulated plastic strain P with:

$$R = \rho_0 \frac{\partial a}{\partial P} \tag{38}$$

$$= BP^n \tag{39}$$

The relation between the kinematic stress tensor $\tilde{\boldsymbol{X}}$, which defines the center of the yield surface in the stress space, and the kinematic hardening variable $\tilde{\boldsymbol{A}}_k$ is:

$$\tilde{\boldsymbol{X}} = \rho_0 \frac{\partial a}{\partial \tilde{\boldsymbol{A}}_k} \tag{40}$$

$$= \mathbb{K} : \tilde{\boldsymbol{A}}_k \tag{41}$$

It is emphasized that, because of the definition of the kinematic hardening variable, the kinematic stress tensor $\tilde{\boldsymbol{X}}$ behaves similarly to the second Piola-Kirchoff stress tensor $\tilde{\boldsymbol{S}}$.

The thermodynamic force driving the development of damage is denoted by $-Y$. This thermodynamic force is given by:

$$-Y = \rho_0 \frac{\partial a}{\partial D} \tag{42}$$

$$= \frac{1}{2} \tilde{\boldsymbol{E}}_e : \frac{\partial \mathbb{L}}{\partial D} : \tilde{\boldsymbol{E}}_e + \frac{1}{2} \tilde{\boldsymbol{A}}_k : \frac{\partial \mathbb{K}}{\partial D} : \tilde{\boldsymbol{A}}_k \tag{43}$$

Because of closure effects, the following cases have to be considered when evaluating the derivative of the stiffness tensor with respect to the damage variable:

$$\frac{\partial \mathbb{L}}{\partial D} = \begin{cases} -\mathbb{L}_u, & \tilde{\boldsymbol{E}}_e : \mathbf{1} \geq 0 \\ -\mathbb{L}_u + \mathbb{P}_s : \mathbb{L}_u : \mathbb{P}_s, & \tilde{\boldsymbol{E}}_e : \mathbf{1} < 0 \end{cases} \tag{44}$$

In a similar fashion, the derivative of the kinematic moduli tensor $\mathbb{K}$ with respect to the damage variable is given by:

$$\frac{\partial \mathbb{K}}{\partial D} = \begin{cases} -\mathbb{K}_u, & \tilde{\boldsymbol{A}}_k : \mathbf{1} \geq 0 \\ -\mathbb{K}_u + \mathbb{P}_s : \mathbb{K}_u : \mathbb{P}_s, & \tilde{\boldsymbol{A}}_k : \mathbf{1} < 0 \end{cases} \tag{45}$$

Finally, the specific entropy s, which is the dual variable of temperature T, is given by:

$$s = -\frac{\partial a}{\partial T} \tag{46}$$

$$\begin{aligned} =& \frac{1}{\rho_0} \tilde{\boldsymbol{E}}_\theta : \left(\frac{\partial \mathbb{L}}{\partial T} : \boldsymbol{\alpha} \left(T - T_0 \right) + \mathbb{L} : \frac{\partial \boldsymbol{\alpha}}{\partial T} \left(T - T_0 \right) + \mathbb{L} : \boldsymbol{\alpha} \right) \\ & - \frac{1}{2\rho_0} \tilde{\boldsymbol{E}}_\theta : \frac{\partial \mathbb{L}}{\partial T} : \tilde{\boldsymbol{E}}_\theta + \left(c_0 - \gamma T_0 \right) \ln \left(\frac{T}{T_0} \right) + \gamma \left(T - T_0 \right) \\ & + \frac{1}{2\rho_0} \left(\frac{\partial \lambda_u}{\partial T} - \frac{\partial \lambda}{\partial T} \right) \left(T - T_0 \right)^2 + \frac{1}{\rho_0} \left(\lambda_u - \lambda \right) \left(T - T_0 \right) \\ & - \frac{1}{\rho_0 \left(n + 1 \right)} \frac{\partial B}{\partial T} P^{n+1} - \frac{1}{2\rho_0} \tilde{\boldsymbol{A}}_k : \frac{\partial \mathbb{K}}{\partial T} : \tilde{\boldsymbol{A}}_k \end{aligned} \tag{47}$$

For the purpose of conciseness, the above state equation for specific entropy uses the variables λ and λ_u that are defined according to:

$$\lambda_u = \boldsymbol{\alpha} : \mathbb{L}_u : \boldsymbol{\alpha} \tag{48}$$

$$\lambda = \boldsymbol{\alpha} : \mathbb{L} : \boldsymbol{\alpha} \tag{49}$$

The list of state equations for the proposed model consists of equations (37), (39), (41), (43) and (47).

2.5. Specific dissipation source

For the evolution of a material point to be compatible with the second law of thermodynamics, the specific dissipation source d must be non-negative.

Using the relation $u = a + sT$, the dissipation inequality (19) becomes:

$$d = \frac{\tilde{\boldsymbol{S}} : \dot{\tilde{\boldsymbol{E}}}_\theta}{\rho_0} + \frac{\tilde{\boldsymbol{\Sigma}} : \tilde{\boldsymbol{L}}_p}{\rho_0} - \dot{a} - s\dot{T} - \frac{1}{\rho_0 T}\tilde{\boldsymbol{Q}} \cdot \tilde{\boldsymbol{\nabla}} T \geq 0 \tag{50}$$

In the following, the distinction is made between the thermal dissipation source d_{th} and the intrinsic dissipation source d_{in}. These two dissipation sources are assumed to be separated in the sense that each of them is required to be non-negative:

$$d_{in} = \frac{\tilde{\boldsymbol{S}} : \dot{\tilde{\boldsymbol{E}}}_\theta}{\rho_0} + \frac{\tilde{\boldsymbol{\Sigma}} : \tilde{\boldsymbol{L}}_p}{\rho_0} - \dot{a} - s\dot{T} \geq 0 \tag{51}$$

$$d_{th} = -\frac{1}{\rho_0 T}\tilde{\boldsymbol{Q}} \cdot \tilde{\boldsymbol{\nabla}} T \geq 0 \tag{52}$$

Using the definitions (36), (38), (40), (42) and (46) of the thermodynamic forces, the time derivative of the specific free energy is expressed by:

$$\dot{a} = \frac{1}{\rho_0}\tilde{\boldsymbol{S}} : \dot{\tilde{\boldsymbol{E}}}_\theta + \frac{1}{\rho_0}\tilde{\boldsymbol{X}} : \dot{\tilde{\boldsymbol{A}}}_k + \frac{1}{\rho_0} R\dot{P} - \frac{1}{\rho_0} Y\dot{D} - s\dot{T} \tag{53}$$

The above expression allows reformulating the specific intrinsic dissipation d_{in} source as follows:

$$d_{in} = \frac{1}{\rho_0}\tilde{\boldsymbol{\Sigma}} : \tilde{\boldsymbol{L}}_p - \frac{1}{\rho_0}\tilde{\boldsymbol{X}} : \dot{\tilde{\boldsymbol{A}}}_k - \frac{1}{\rho_0} R\dot{P} + \frac{1}{\rho_0} Y\dot{D} \tag{54}$$

For the construction of a yield criterion, it is necessary to define a kinematic stress tensor that behaves like $\tilde{\boldsymbol{\Sigma}}$. For this purpose, it is worth mentioning that the Mandel stress tensor $\tilde{\boldsymbol{\Sigma}}$ is connected to the second Piola-Kirchoff stress tensor $\tilde{\boldsymbol{S}}$ with:

$$\tilde{\boldsymbol{\Sigma}} = \boldsymbol{F}_\theta^T \cdot \boldsymbol{F}_\theta \cdot \tilde{\boldsymbol{S}} \tag{55}$$

Guided by the above relation, the following Mandel stress-like tensor $\tilde{\boldsymbol{\chi}}$ is introduced:

$$\tilde{\boldsymbol{\chi}} = \boldsymbol{F}_\theta^T \cdot \boldsymbol{F}_\theta \cdot \tilde{\boldsymbol{X}} \tag{56}$$

This definition of the kinematic stress tensor $\tilde{\boldsymbol{\chi}}$ leads to the following expression of the intrinsic dissipation source:

$$d_{in} = \frac{1}{\rho_0}\tilde{\boldsymbol{\Sigma}} : \tilde{\boldsymbol{L}}_p - \frac{1}{\rho_0}\tilde{\boldsymbol{\chi}} : \tilde{\boldsymbol{L}}_k - \frac{1}{\rho_0} R\dot{P} + \frac{1}{\rho_0} Y\dot{D} \tag{57}$$

with:

$$\tilde{\boldsymbol{L}}_k = \boldsymbol{F}_\theta^{-1} \cdot \boldsymbol{F}_\theta^{-T} \cdot \dot{\tilde{\boldsymbol{A}}}_k \tag{58}$$

Expressions (52) and (57) emphasize that, for the constitutive model to be complete, some evolution rules for $\tilde{\boldsymbol{L}}_p$, $\tilde{\boldsymbol{L}}_k$, $\dot{P}$, $\dot{D}$ and $\tilde{\boldsymbol{Q}}$ must be proposed, with the restriction that the specific intrinsic and thermal dissipation sources remain non-negative.

2.6. Evolution equations

Fourier's law of heat conduction. According to Fourier's law of heat conduction, the constitutive relation for the heat flux density vector $\tilde{\boldsymbol{Q}}$ is:

$$\tilde{\boldsymbol{Q}} = -\boldsymbol{\kappa} \cdot \tilde{\boldsymbol{\nabla}} T \tag{59}$$

where $\boldsymbol{\kappa}$ is the thermal conductivity tensor, which has to be positive-definite for the thermal dissipation source d_{th} to be non-negative. The influence of temperature and damage on the thermal conductivity tensor is modelled with:

$$\boldsymbol{\kappa} = \boldsymbol{\kappa}_0 \left(1 + \vartheta \left(T - T_0\right)\right) \left(1 - D\right) \tag{60}$$

where $\boldsymbol{\kappa}_0$ is the thermal conductivity tensor at the reference temperature and ϑ is a material parameter.

Viscoplastic flow rule. For the construction of the plastic flow rule, it is convenient to introduce a scalar function ϕ that allows determining an equivalent stress Σ_{eq} such that:

$$\Sigma_{eq} = \phi \left[\tilde{\boldsymbol{\Sigma}}_d - \tilde{\boldsymbol{\chi}}_d\right] \tag{61}$$

Because plastic flow is assumed to be incompressible (i.e. $\tilde{\boldsymbol{L}}_p : \mathbf{1} = 0$), the equivalent stress solely depends on the deviatoric parts $\tilde{\boldsymbol{\Sigma}}_d$ and $\tilde{\boldsymbol{\chi}}_d$ of the applied and kinematic stress tensors $\tilde{\boldsymbol{\Sigma}}$ and $\tilde{\boldsymbol{\chi}}$. The deviatoric stress tensors $\tilde{\boldsymbol{\Sigma}}_d$ and $\tilde{\boldsymbol{\chi}}_d$ are given by:

$$\tilde{\boldsymbol{\Sigma}}_d = \tilde{\boldsymbol{\Sigma}} - \mathbb{P}_s : \tilde{\boldsymbol{\Sigma}} = \mathbb{P}_d : \tilde{\boldsymbol{\Sigma}} \tag{62}$$

$$\tilde{\boldsymbol{\chi}}_d = \tilde{\boldsymbol{\chi}} - \mathbb{P}_s : \tilde{\boldsymbol{\chi}} = \mathbb{P}_d : \tilde{\boldsymbol{\chi}} \tag{63}$$

where $\mathbb{P}_d = \mathbb{I} - \mathbb{P}_s$ is the deviatoric projection tensor.

If the normality rule is adopted, the evolution laws for $\tilde{\boldsymbol{L}}_p$ and $\tilde{\boldsymbol{L}}_k$ have the following form:

$$\tilde{\boldsymbol{L}}_p = \dot{P}\frac{\partial \phi}{\partial \tilde{\boldsymbol{\Sigma}}} = \dot{P}\frac{\partial \phi}{\partial \tilde{\boldsymbol{\Sigma}}_d} : \mathbb{P}_d \tag{64}$$

$$\tilde{\boldsymbol{L}}_k = -\dot{P}\frac{\partial \phi}{\partial \tilde{\boldsymbol{\chi}}} = -\dot{P}\frac{\partial \phi}{\partial \tilde{\boldsymbol{\chi}}_d} : \mathbb{P}_d \tag{65}$$

Since the equivalent stress depends only on the difference between $\tilde{\boldsymbol{\Sigma}}_d$ and $\tilde{\boldsymbol{\chi}}_d$, we have[1]:

$$\frac{\partial \phi}{\partial \tilde{\boldsymbol{\Sigma}}} = -\frac{\partial \phi}{\partial \tilde{\boldsymbol{\chi}}} = \boldsymbol{N} \tag{66}$$

where $\boldsymbol{N}$ is the plastic flow direction. Using the above definition of the plastic flow direction, one obtains:

$$\tilde{\boldsymbol{L}}_k = \tilde{\boldsymbol{L}}_p = \dot{P}\boldsymbol{N} \tag{67}$$

Also, because ϕ is a homogeneous function of degree one, the application of Euler's homogeneous function theorem leads to:

$$\left(\tilde{\boldsymbol{\Sigma}} - \tilde{\boldsymbol{\chi}}\right) : \boldsymbol{N} = \Sigma_{eq} \tag{68}$$

Using the above property, the expression of the intrinsic dissipation source d_{in} reduces to:

$$d_{in} = \frac{1}{\rho_0}\left(\Sigma_{eq} - R\right)\dot{P} + \frac{1}{\rho_0} Y \dot{D} \tag{69}$$

Because the equivalent plastic strain rate $\dot{P}$ is non-negative, the following conditions must hold for the intrinsic dissipation source to be non-negative:

$$\begin{cases} \dot{P} = 0, & \Sigma_{eq} < R \\ \dot{P} \geq 0, & \Sigma_{eq} \geq R \end{cases} \tag{70}$$

[1]For isotropic materials, the Mandel stress tensor $\tilde{\boldsymbol{\Sigma}}$ is symmetric (Gurtin et al., 2010). For this specific case, the plastic flow is irrotational in the sense that, due to the adoption of the normality rule, the plastic contribution to the velocity gradient tensor $\tilde{\boldsymbol{L}}_p$ is symmetric as well.

Prior to discussing the possible choices for the evolution equation for $\dot{P}$, usually known as the viscoplastic flow rule, the yield stress Σ_y of a material point is defined according to:

$$\Sigma_y = A + R \tag{71}$$

where A represents the initial yield stress, i.e. when no plastic strain has been accumulated yet. The initial yield stress A is usually very dependent on the absolute temperature. To include this dependence of A with respect to temperature, a similar relation to that of B is used. As a result, the following options for the initial yield stress are considered:

$$A = A_0 \left(1 - \left(\frac{T - T_0}{T_M - T_0} \right)^m \right) \tag{72a}$$

$$A = A_0 \left(1 - \frac{T^m - T_0^m}{T_M^m - T_0^m} \right) \tag{72b}$$

where A_0 is the yield stress at the reference temperature. According to the state equation (39), the yield stress is therefore given by either one or the other following relations:

$$\Sigma_y = (A_0 + B_0 P^n) \left(1 - \left(\frac{T - T_0}{T_M - T_0} \right)^m \right) \tag{73a}$$

$$\Sigma_y = (A_0 + B_0 P^n) \left(1 - \frac{T^m - T_0^m}{T_M^m - T_0^m} \right) \tag{73b}$$

A stronger requirement than (70) consists in assuming that no plastic flow can occur when the equivalent stress Σ_{eq} is inferior to the yield stress Σ_y, that is:

$$\begin{cases} \dot{P} = 0, & \Sigma_{eq} < \Sigma_y \\ \dot{P} \geq 0, & \Sigma_{eq} \geq \Sigma_y \end{cases} \tag{74}$$

In the present work, two different possibilities are considered for the construction of the viscoplastic flow rule:

$$\dot{P} = \begin{cases} 0, & \Sigma_{eq} < \Sigma_y \\ \dot{P}_0 \exp\left(\frac{\Sigma_{eq}}{C\Sigma_y} - \frac{1}{C} \right), & \Sigma_{eq} \geq \Sigma_y \end{cases} \tag{75a}$$

$$\dot{P} = \begin{cases} 0, & \Sigma_{eq} < \Sigma_y \\ \dot{P}_0 \exp\left(\frac{\Sigma_{eq}}{C\Sigma_y} - \frac{1}{C} \right) - \dot{P}_0, & \Sigma_{eq} \geq \Sigma_y \end{cases} \tag{75b}$$

where C is a material parameter and $\dot{P}_0$ is a reference strain rate. The flow rule (75a) corresponds to the original proposition of Johnson and Cook (1983). It is clear that, when the conditions for plastic flow are met (i.e. $\Sigma_{eq} \geq \Sigma_y$), the minimum value of the equivalent plastic strain rate is $\dot{P}_0$. The Johnson-Cook model is therefore not applicable for low strain rates (i.e. $\dot{P} < \dot{P}_0$). Also, the equivalent plastic strain rate is a discontinuous function of Σ_{eq}/Σ_y, which may give rise to a non-smooth elastic-plastic transition. To circumvent these limitations, an alternative flow rule, given by equation (75b), is proposed. As illustrated by Figure 1, for large strain rates (i.e. when $\dot{P}/\dot{P}_0 \gg 1$), this alternative flow rule is quasi-identical to the original Johnson-Cook model. For low strain rates, the modified Johnson-Cook model of Camacho and Ortiz (1997) is retrieved.

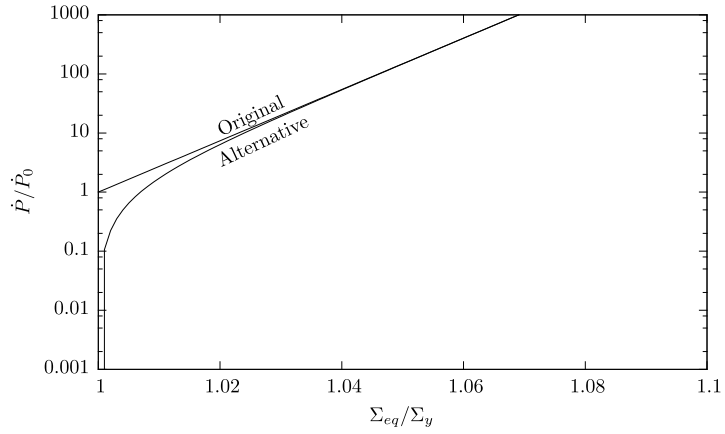

Figure 1: Comparison between the original and alternative viscoplastic flow rules. For the present comparison, the C parameter is set to 0.01.

The classical presentation of the Johnson-Cook constitutive model is obtained from the definition of the yield stress (73) and the flow rule (75). Depending on the chosen flow rule and yield stress definition, one has:

$$\Sigma_{eq} = (A_0 + B_0 P^n)\left(1 + C\ln\left(\frac{\dot{P}}{\dot{P}_0}\right)\right)\left(1 - \left(\frac{T - T_0}{T_M - T_0}\right)^m\right), \dot{P} \geq \dot{P}_0 \quad (76a)$$

$$\Sigma_{eq} = (A_0 + B_0 P^n)\left(1 + C\ln\left(1 + \frac{\dot{P}}{\dot{P}_0}\right)\right)\left(1 - \frac{T^m - T_0^m}{T_M^m - T_0^m}\right), \dot{P} > 0 \quad (76b)$$

The original Johnson-Cook model, which results from the combination of equations (73a) and (75a), is given by (76a). An alternative Johnson-Cook

model, which has been obtained from equations (73b) and (75b), is provided by equation (76b). These models will be compared with each other in the next section.

Damage rule. According to the Johnson and Cook (1985) ductile fracture criterion, fracture occurs when the equivalent plastic strain P reaches a critical value P_f. The critical value P_f, which can be interpreted as an equivalent fracture strain, depends on the equivalent strain rate $\dot{P}$, the temperature T and the triaxiality ratio τ:

$$P_f = \left(D_1 + D_2 \exp\left(D_3 \tau\right)\right) \left(1 + D_4 \ln\left(\frac{\dot{P}}{\dot{P}_0}\right)\right) \left(1 + D_5 \frac{T - T_0}{T_M - T_0}\right) \tag{77}$$

where D_1, D_2, D_3 ,D_4 and D_5 are material parameters. The triaxiality ratio τ is given by the ratio between the hydrostatic stress and the von Mises equivalent stress:

$$\tau = \frac{1}{3} \frac{\boldsymbol{\Sigma} : \mathbf{1}}{\sqrt{\frac{3}{2} \boldsymbol{\Sigma}_d : \boldsymbol{\Sigma}_d}} \tag{78}$$

In the general case, the fracture strain P_f is not constant during a deformation process. It is however possible to determine whether the conditions for ductile fracture are met or not by introducing a damage variable H. Assuming a linear cumulative damage rule, the evolution of the damage variable H is given by:

$$\dot{H} = \frac{\dot{P}}{P_f} \tag{79}$$

It should be noticed that, in contrast with D, the damage variable H has no influence on material properties. To account for the stiffness degradation caused by the development of ductile damage, the following damage rule is used:

$$\dot{D} = \begin{cases} 0, & H < 1 \text{ or } Y < 0 \\ \left(\frac{H-1}{G}\right)^z (1 - D), & H \geq 1 \text{ and } Y \geq 0 \end{cases} \tag{80}$$

According to the above equation, the damage variable D increases if and only if the conditions for ductile fracture are met (i.e. $H \geq 1$). Also, as shown by equation (57), the progression of damage contributes to the intrinsic dissipation source. For this contribution to be non-negative, damage is allowed to

grow if and only if the corresponding driving force Y is non-negative[2]. For a given material, the progression of the damage variable can be adjusted with the G and z material parameters.

2.7. Heat diffusion equation

The proposed Johnson-Cook model consists of the state equations (37), (39), (41), (43) and (47), the equivalent stress definition (61) and the evolution equations (59), (64), (65), (75) and (80). To understand the implications of the thermomechanical couplings that are considered in the constitutive model, it is instructive to derive the heat diffusion equation. According the first law of thermodynamics, we have:

$$\dot{u} = \dot{a} + \dot{s}T + s\dot{T} = \frac{1}{\rho}\boldsymbol{\sigma} : \boldsymbol{L} + r - \boldsymbol{\nabla} \cdot \boldsymbol{q} \tag{81}$$

From the definition (51) of the specific intrinsic dissipation source d_{in}, one obtains:

$$\dot{s}T = d_{in} + r - \boldsymbol{\nabla} \cdot \boldsymbol{q} \tag{82}$$

Using the state equation (47) for the specific entropy s, the left-hand term of the above equation becomes:

$$\dot{s}T = T\frac{\partial s}{\partial \tilde{\boldsymbol{E}}_\theta} : \dot{\tilde{\boldsymbol{E}}}_\theta + T\frac{\partial s}{\partial \tilde{\boldsymbol{A}}_k} : \dot{\tilde{\boldsymbol{A}}}_k + T\frac{\partial s}{\partial P}\dot{P} + T\frac{\partial s}{\partial D}\dot{D} + T\frac{\partial s}{\partial T}\dot{T} \tag{83}$$

Combining equations (82) and (83) leads to the following form of the heat diffusion equation:

$$c\dot{T} = d_{in} + \varphi_\theta + \varphi_{ic} + r - \boldsymbol{\nabla} \cdot \boldsymbol{q} \tag{84}$$

According to the above equation, different heat sources control the temperature evolution of a material point. The thermoelastic heat source φ_θ is:

$$\varphi_\theta = -T\frac{\partial s}{\partial \tilde{\boldsymbol{E}}_\theta} : \dot{\tilde{\boldsymbol{E}}}_\theta \tag{85}$$

$$= \frac{1}{\rho_0}T\left(\frac{\partial \mathbb{L}}{\partial T} : \tilde{\boldsymbol{E}}_\theta - \left(\frac{\partial \mathbb{L}}{\partial T} : \boldsymbol{\alpha} + \mathbb{L} : \frac{\partial \boldsymbol{\alpha}}{\partial T}\right)(T - T_0) - \mathbb{L} : \boldsymbol{\alpha}\right) : \dot{\tilde{\boldsymbol{E}}}_\theta \tag{86}$$

[2]For isotropic and cubic materials, Y is necessarily non-negative, in which case the evolution law for the damage variable D solely depends on H.

The specific heat source resulting from the couplings between internal (i.e. hardening and damage) variables and temperature φ_{ic} is given by:

$$\begin{aligned}\varphi_{ic} =& -T\frac{\partial s}{\partial \tilde{\boldsymbol{A}}_k} : \dot{\tilde{\boldsymbol{A}}}_k - T\frac{\partial s}{\partial P}\dot{P} - T\frac{\partial s}{\partial D}\dot{D} && (87)\\ =& \frac{1}{\rho_0}T\tilde{\boldsymbol{A}}_k : \frac{\partial \mathbb{K}}{\partial T} : \dot{\tilde{\boldsymbol{A}}}_k + \frac{1}{\rho_0}T\frac{\partial B}{\partial T}P^n\dot{P} \\ &+ \frac{1}{2\rho_0}T\left(\tilde{\boldsymbol{E}}_e : \frac{\partial^2 \mathbb{L}}{\partial T \partial D} : \tilde{\boldsymbol{E}}_e + \tilde{\boldsymbol{A}}_k : \frac{\partial^2 \mathbb{K}}{\partial T \partial D} : \tilde{\boldsymbol{A}}_k\right)\dot{D} && (88)\\ &- \frac{1}{\rho_0}T\tilde{\boldsymbol{E}}_e : \frac{\partial \mathbb{L}}{\partial D} : \left(\frac{\partial \boldsymbol{\alpha}}{\partial T}\left(T - T_0\right) + \boldsymbol{\alpha}\right)\dot{D}\end{aligned}$$

Finally, the specific heat capacity c is given by:

$$\begin{aligned}c =& T\frac{\partial s}{\partial T} && (89)\\ =& \frac{1}{\rho_0}2T\tilde{\boldsymbol{E}}_\theta : \left(\frac{\partial \mathbb{L}}{\partial T} : \boldsymbol{\alpha} + \mathbb{L} : \frac{\partial \boldsymbol{\alpha}}{\partial T} + \frac{\partial \mathbb{L}}{\partial T} : \frac{\partial \boldsymbol{\alpha}}{\partial T}\left(T - T_0\right)\right) \\ &+ \frac{1}{2\rho_0}T\left(\frac{\partial^2 \lambda_u}{\partial T^2} - \frac{\partial^2 \lambda}{\partial T^2}\right)\left(T - T_0\right)^2 + \frac{2}{\rho_0}T\left(\frac{\partial \lambda_u}{\partial T} - \frac{\partial \lambda}{\partial T}\right)\left(T - T_0\right) && (90)\\ &+ \frac{1}{\rho_0}T\left(\lambda_u - \lambda\right) + c_0 + \gamma\left(T - T_0\right) - T\frac{1}{\rho_0}\frac{\partial^2 B}{\partial T^2}\frac{P^{n+1}}{n+1}\end{aligned}$$

It is emphasized that, due to the impact of temperature on the stiffness and thermal expansion properties and the isotropic hardening modulus, the specific heat capacity c depends on both the thermoelastic strain tensor $\tilde{\boldsymbol{E}}_\theta$ and the equivalent plastic strain P. Also, depending on the retained option, it is worth mentioning that the second derivative of B with respect to temperature is:

$$\begin{aligned}\frac{\partial^2 B}{\partial T^2} &= -B_0 m\left(m-1\right)\left(T - T_0\right)^{m-2}\left(T_M - T_0\right)^{-m} && (91a)\\ \frac{\partial^2 B}{\partial T^2} &= -B_0 m\left(m-1\right)T^{m-2}\left(T_M^m - T_0^m\right)^{-1} && (91b)\end{aligned}$$

According to equation (91a), this derivative does not necessarily exist for $T = T_0$ when $m < 2$ and $m \neq 1$, in which case the specific heat capacity cannot be evaluated. The classical formulation of the Johnson-Cook model should therefore be used with caution for coupled thermomechanical problems.

As shown by equation (84), the construction of the heat diffusion equation does not require the introduction of the so-called Taylor-Quinney coefficient (Taylor and Quinney, 1934). Indeed, this coefficient, which measures the fraction of plastic work rate being dissipated into heat, is entirely determined by constitutive relations. In constrast with some studies considering this coefficient as a constant material parameter (Børvik et al., 2001; Su and Stainier, 2015), the present approach is consistent with the experimental observations showing that it depends on both the loading conditions and deformation history (Rittel, 1999).

3. Illustrative examples

In this section, the proposed set of constitutive equations is used to model the behaviour of a 4340 steel. The corresponding material parameters are listed in Table 1. Both the mechanical and thermophysical properties are assumed to be isotropic. The parameters of the Johnson-Cook model, for both the viscoplastic flow rule and the damage rule, have been obtained by Johnson and Cook (1985). The reference equivalent plastic strain rate $\dot{P}_0$ and temperature T_0 are respectively fixed to 1 s^{-1} and 293 K. For simplicity, the variation of the thermal expansion coefficient, thermal conductivity and heat capacity with respect to temperature are not considered. The von Mises yield criterion is used for all the following examples. Except for the specific case of a Bauschinger test (see below), kinematic hardening is not considered.

3.1. Isothermal tension tests

To compare the original and alternative formulations of the Johnson-Cook model, the specific case of uniaxial tension is first considered. The loading conditions are such that both the temperature T and the axial logarithmic strain rate $\dot{\epsilon}$ are constant. The axial Cauchy stress σ is plotted as a function of the axial logarithmic strain ϵ for different strain rates and different temperatures in Figure 2. According to the results, only minor differences between both formulations are observed, even for low strain rates (i.e. when $\dot{P} \approx \dot{P}_0$). This indicates that the original and alternative formulations of the Johnson-Cook model are very similar, but only the alternative formulation allows extrapolating to either low strain rates (i.e. $\dot{P} < \dot{P}_0$) or low temperatures (i.e. $T < T_0$).

	Parameters				
Physical	ρ_0	c_0	γ	T_M	
	7830 kg/m^3	477 J/kg/K	0 K^{-1}	1793 K	
Heat conduction	κ_0	θ			
	37 W/m/K	0 K^{-1}			
Thermoelastic	E_0	ν	α_0	β	ζ
	200 GPa	0.29	11 MK^{-1}	0.00047 K^{-1}	0 K^{-1}
Viscoplastic	A_0	B_0	C	n	m
	792 MPa	510 MPa	0.014	0.26	1.03
Damage	D_1	D_2	D_3	D_4	D_5
	0.05	3.44	-2.12	0.002	0.61
	G	z			
	0.01 MPa	10			

Table 1: Material parameters used for the application of the Johnson-Cook constitutive model.

3.2. Adiabatic tension tests

To evaluate the relative importance of the different heat sources, the case of an adiabatic uniaxial tension test is now examined. The initial temperature T is set to 293 K and the axial logarithmic strain rate $\dot{\epsilon}$ is equal to 1 s^{-1}. The evolutions of the axial stress σ and the absolute temperature T as a function of the axial logarithmic strain ϵ, which have been obtained from the alternative Johnson-Cook model, are displayed in Figure 3. The contributions of the different heat sources to the temperature evolution are plotted in Figure 4. According to the results, except for the final stage of damage growth, the contribution of the thermoelastic source φ_θ is relatively small. It can thus be neglected for most practical applications. Nevertheless, prior to total failure, the thermoelastic contribution varies significantly. Indeed, during the final deformation stage, the applied stress is too low for plastic deformation to occur. As a result, since further plastic deformation is almost impossible, the thermoelastic strain rate increases when damage becomes significant. As indicated by Equation (86), this causes a rapid variation of the thermoelastic source. Also, though the intrinsic dissipation source d_{in} provides the most important contribution, the temperature evolution is significantly impacted by the internal coupling source φ_{ic}. The importance of the internal coupling source, which should therefore be considered for thermomechanical problems, has also been highlighted by Ranc and Chrysochoos

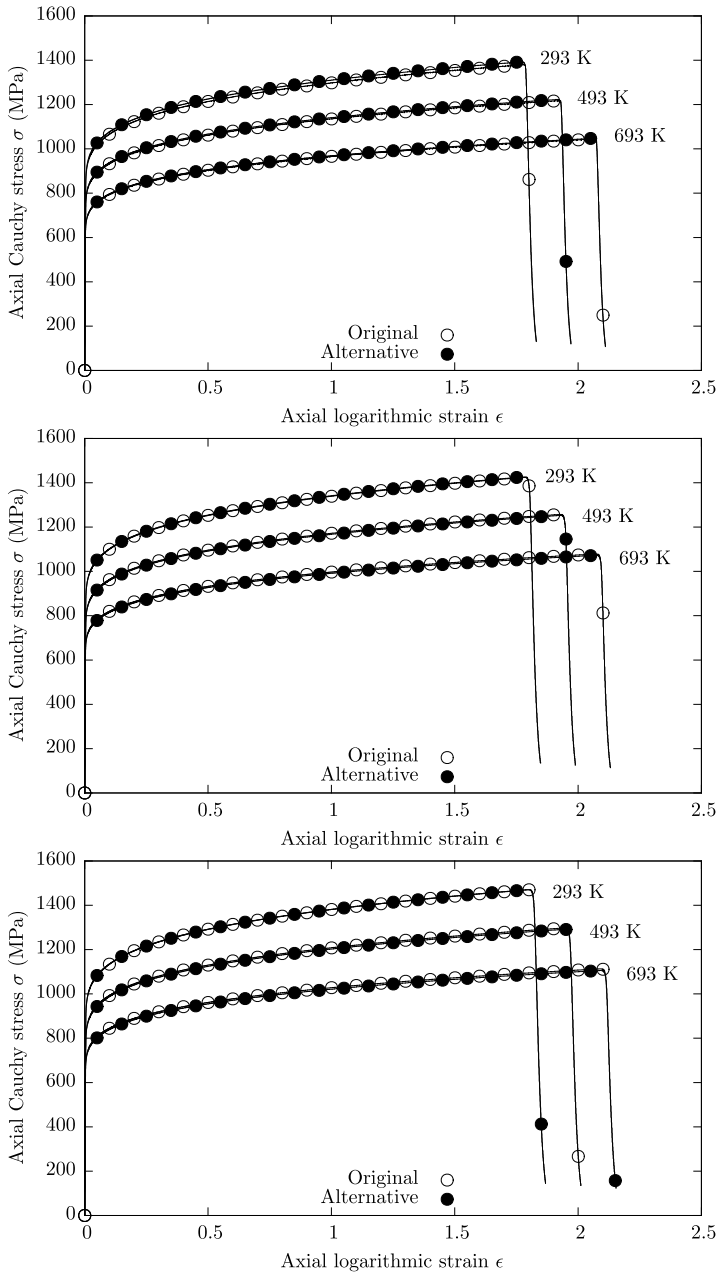

Figure 2: Evolution of the axial Cauchy stress σ as a function of the axial logarithmic strain ϵ during an isothermal uniaxial tension tests for different strain rates: 1 s^{-1} (top), 10 s^{-1} (middle) and 100 s^{-1} (bottom).

(2013).

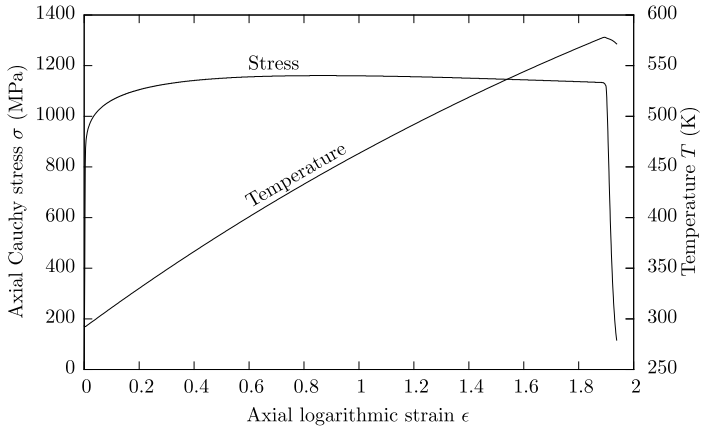

Figure 3: Evolution of the axial Cauchy stress σ and absolute temperature T as a function of the axial logarithmic strain ϵ during an adiabatic uniaxial tension test for a strain rate of 1 s^{-1} and an initial temperature of 293 K.

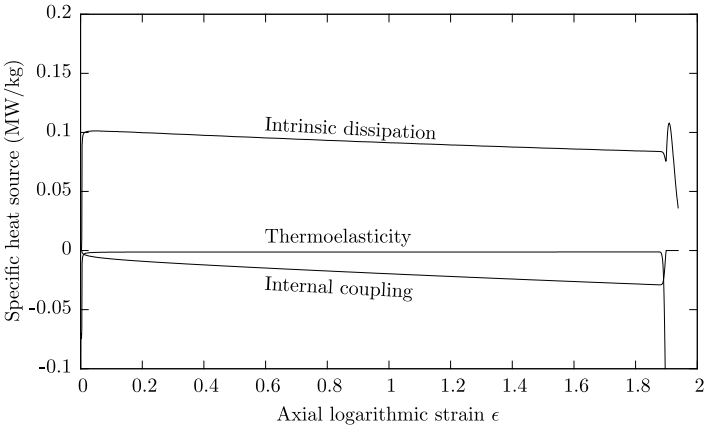

Figure 4: Evolution of the different heat sources as a function of the axial logarithmic strain ϵ during an adiabatic uniaxial tension test for a strain rate of 1 s^{-1} and an initial temperature of 293 K.

3.3. Bauschinger tests

For the purpose of evaluating the impact of kinematic hardening on the flow behaviour, the alternative Johnson-Cook model is used to evaluate the response of a material point during a Bauschinger test. In the present case,

the Bauschinger test consists in first performing an isothermal shear test, up to a shear strain γ of 10%, with a shear strain rate $\dot{\gamma}$ of 1 s^{-1}. The loading direction is then reversed (i.e. $\dot{\gamma} = -1$ s^{-1}) until the shear strain γ vanishes.

To limit the number of material parameters, the initial kinematic hardening moduli tensor $\mathbb{K}_0$ is assumed to be equal to some fraction ξ of the initial elastic stiffness tensor $\mathbb{L}_0$, that is:

$$\mathbb{K}_0 = \xi \, \mathbb{L}_0 \tag{92}$$

The absence of kinematic hardening corresponds to the situation where ξ is equal to zero. The evolution of the shear stress τ as a function of the shear strain γ is presented in Figure 5 for different values of ξ. The results show how the ξ parameter allows controlling the translation of yield surface in the stress space.

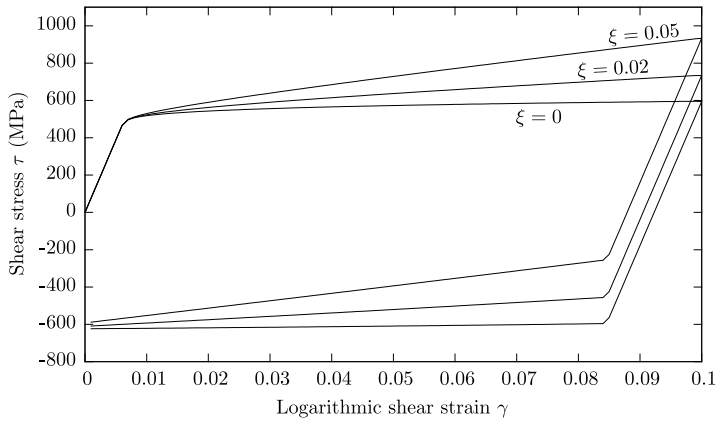

Figure 5: Evolution of the shear stress τ as a function of the logarithmic shear strain γ during an isothermal Bauschinger test for a shear strain rate of ± 1 s^{-1} and a temperature of 293 K.

3.4. Charpy impact test

For the next application, a notched specimen, whose geometry is presented in Figure 6, is subjected to an adiabatic impact test. The velocity of the striker is set to 5 $m{\cdot}s^{-1}$. For the resolution of the field equations resulting from equilibrium and compatibility conditions, the ABAQUS explicit finite element solver is used. Both the striker and the support are modelled as analytical rigid surfaces while the specimen is meshed with C3D8R elements. The friction coefficient between the specimen and both the striker and the

support is fixed to 0.3. Elements for which the damage variable D of the corresponding integration points has reached a unit value are deleted.

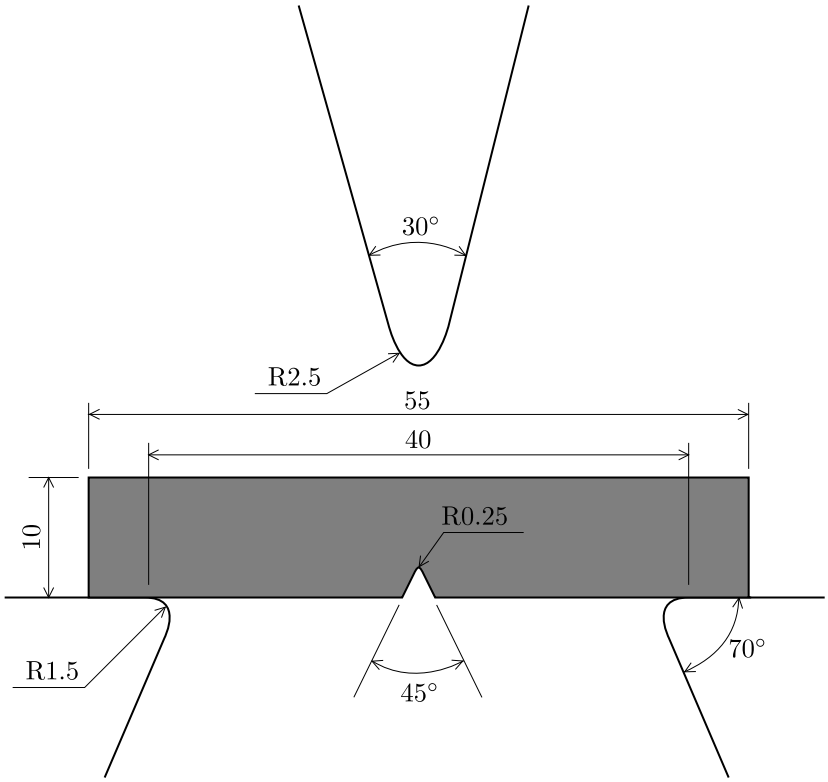

Figure 6: Geometries of the notched specimen, striker and support used for the simulation of a Charpy Impact test.

The evolution of the equivalent plastic strain field P is presented in Figure 7. As experimentally observed, the crack initiates from the notch and propagates toward the upper surface of the specimen. Also, because the proposed model has been developed within a consistent thermodynamic framework, the partition of energy during a thermomechanical process can be investigated. The partition of the total work into dissipated and internal energies during impact is presented in Figure 8. According to the results, most of the total work developed by external forces is dissipated into heat, essentially as a result of intrinsic dissipation. Nevertheless, the increase of total internal energy indicates that an important part of the total work is stored within the specimen because of the microstructural transformations (e.g. hardening) occuring during the deformation process.

3.5. Quenching

The last application aims at demonstrating the interest of the proposed model for thermomechanical problems. For this purpose, the impact of a thermal loading on the formation of residual stresses is investigated. Specifically, the alternative Johnson-Cook model is used to determine the residual stress field resulting from the quenching of a cylindrical specimen. The dimensions of the cylindrical specimen, together with the boundary conditions, are given in Figure 9. For the application of the thermal load, the temperature history is prescribed on the external surface. It consists of cooling the specimen from 893 K to 293 K with a cooling rate of 100 $\mathrm{K{\cdot}s^{-1}}$. The temperature is then held constant until thermal equilibrium is reached. As before, the ABAQUS explicit finite element solver is used for the resolution of field equations. Because of symmetry planes, only one eighth of the specimen is considered for the finite element model. The specimen is meshed with C3D8T elements, for which the nodal variables are the three components of the displacement vector and the temperature.

As shown in Figure 10, important temperature gradients due to the high cooling rate produce an internal stress field. The internal stress field allows the accumulation of plastic strains near the external surface. Though the magnitude of plastic strains is rather small (about 3×10^{-3}), the plastic strain field is responsible for the formation of important residual stresses, which can be observed once thermal equilibrium has been reached (at $t = 600$ s).

4. Conclusion

In this work, the Johnson-Cook model, which is widely used for the description of the mechanical behavior under severe loading conditions, has been revisited from the point of view of thermodynamics with internal variables. Specifically, to construct a thermomechanical constitutive model, some internal state variables have been introduced to consider both isotropic hardening, kinematic hardening and ductile damage. These internal state variables have then been used to propose a definition of the specific free energy, whose derivation has lead to the state equations governing the behaviour of a material point. From the expression of the specific dissipation source, the dissipative forces controlling the evolution of the internal variables have been identified. Some evolution equations, which include the viscoplastic flow rule of Johnson and Cook (1983), have been detailed. Such evolution equations, when associated with state equations, form a complete thermomechanical

constitutive model. Finally, the constitutive relations have been used to obtain the expressions of the different heat sources involved in the heat diffusion equation.

When constructing the constitutive model, some alternative options have been explored for the definition of the thermal softening function and the viscoplastic flow rule. As shown by some illustrative examples, these alternative options provide a description of the mechanical behaviour that is quite similar to the original Johnson-Cook model. Nevertheless, these alternative options allow circumventing the difficulties associated with the definition of the specific heat capacity and the validity of the flow rule at low strain rates and low temperatures.

References

Agmell, M., Ahadi, A., Ståhl, J.E., 2014. Identification of plasticity constants from orthogonal cutting and inverse analysis. Mechanics of Materials 77, 43–51. https://doi.org/10.1016/j.mechmat.2014.07.005.

Børvik, T., Hopperstad, O.S., Berstad, T., Langseth, M. 2001. A computational model of viscoplasticity and ductile damage for impact and penetration. Eur. J. Mech. A/Solids 20, 685–712.

Camacho, G.T., Ortiz, M., 1997. Adaptive Lagrangian modelling of ballistic penetration of metallic targets. Int. J. Comp. Meth. Appl. Mech. Engng. 142, 269–301.

Chen, G., Ren, C., Ke, Z., Li, J., Yang, X., 2016. Modeling of flow behavior for 7050-T7451 aluminum alloy considering microstructural evolution over a wide range of strain rates. Mechanics of Materials 95, 146–157. https://doi.org/10.1016/j.mechmat.2016.01.006.

Couque, H., Boulanger, R., Bornet, F., 2006. A modified Johnson-Cook model for strain rates ranging from 10^{-3} to 10^{5} s^{-1}. J. Phys. IV France 134, 87–93.

Djavanroodi, F., Hussain, Z., Irfan, O.M., Al-Mufadi, F., 2019. Strain Behavior of Nickel Alloy 200 during Multiaxial Forging through Finite Element Modeling. Metals 9, 1–12. https://doi.org/10.3390/met9020132.

Gurtin, M.E., Fried, E., Anand, L., 2010. The Mechanics and Thermodynamics of Continua. Cambridge University Press, New York.

Hor, A., Morel, F., Lebrun, J.L., Germain, G., 2013. Modelling, identification and application of phenomenological constitutive laws over a large strain rate and temperature range. Mechanics of Materials 64, 91–110. https://doi.org/10.1016/j.mechmat.2013.05.002.

He, A., Xie, G., Zhang, H., Wang, K., 2013. A comparative study on JohnsonCook, modified JohnsonCook and Arrhenius-type constitutive models to predict the high temperature flow stress in 20CrMo alloy steel. Materials and Design 52, 677–685. https://doi.org/10.1016/j.matdes.2013.06.010.

Johnson, G., Cook, W., 1983. A constitutive model and data for metals subjected to large strains, high strain rates, and high temperatures. In: Proc. 7th Int. Symposium on Ballistics, page 541.

Johnson, G., Cook, W., 1985. Fracture characteristics of three metals subjected to various strains, strain rates, temperatures, and pressures. Engineering Fracture Mechanics 21, 31–48.

Lee, E.H., 1969. Elastic Plastic Deformations at Finite Strains. J. appl. Mech. 36.

Mandel, J., 1973. Thermodynamics and plasticity. In: Delgado Domingas, J. J., Nina, M. N.R., Whitelaw, J.H., (Eds.), Proceedings of The International Symposium on Foundations of Continuum Thermodynamics, Halsted Press, New York, 283–304.

Maugin, G.A., Muschik, W., 1994. Thermodynamics with Internal Variables. Part I. General Concepts. J. Non-Equilib. Thermodyn. 19, 217–249.

Ranc, N., Chrysochoos, A., 2013. Calorimetric consequences of thermal softening in JohnsonCooks model. Mechanics of Materials 65, 44–55. https://doi.org/10.1016/j.mechmat.2013.05.007.

Rittel, D., 1999. On the conversion of plastic work to heat during high strain rate deformation of glassy polymers. Mechanics of Materials 31, 131–139.

Shrot, A., Bäker, M., 2012. Determination of Johnson-Cook parameters from machining simulations. Computational Materials Science 52, 298–304. https://doi.org/10.1016/j.commatsci.2011.07.035.

Su, S., Stainier, L., 2015. Energy-based variational modeling of adiabatic shear bands structure evolution. Mechanics of Materials 80, 219–233. https://doi.org/10.1016/j.mechmat.2014.04.013.

Taylor, G.I., Quinney, H., 1934. The latent energy remaining in a metal after cold working. Proc. R. Soc. A143, 307–326.

Umbrello, D., M'Saoubi, R., Outeiro, J.C., 2007. The influence of Johnson-Cook material constants on finite element simulation of machining of AISI 316L steel. International Journal of Machine Tools and Manufacture 47, 462–470. https://doi.org/10.1016/j.ijmachtools.2006.06.006.

Wang, S., Huang Y., Xiao, Z., Liu, Y., Liu, H., 2017. A Modified Johnson-Cook Model for Hot Deformation Behavior of 35CrMo Steel. Metals 7, 1–10. https://doi.org/10.3390/met7090337.

Yoo, Y.H., Yang, D.Y., 1997. Finite element modelling of the high-velocity impact forging process by the explicit time integration method. Journal of Materials Processing Technology 63, 718–723. https://doi.org/10.1016/S0924-0136(96)02713-6.

Zhao, Y., Sun, J., Li, J., Yan, Y., Wang, P., 2017. A comparative study on Johnson-Cook and modified Johnson-Cook constitutive material model to predict the dynamic behavior laser additive manufacturing FeCr alloy. Journal of Alloys and Compounds 723, 179–187. http://dx.doi.org/10.1016/j.jallcom.2017.06.251

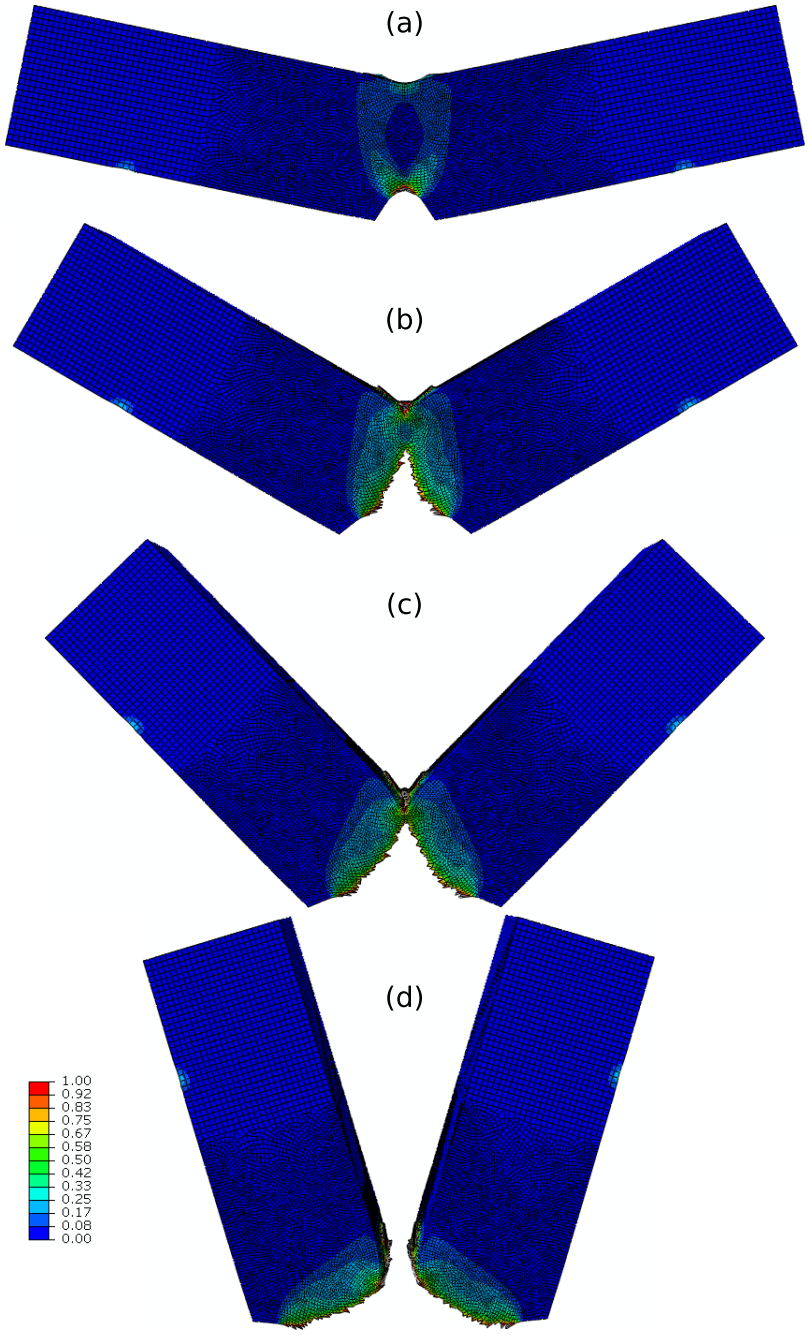

Figure 7: Evolution of the equivalent plastic strain field P during a Charpy impact test: $t = 0.001$ s (a), $t = 0.002$ s (b), $t = 0.003$ s (c) and $t = 0.006$ s (d).

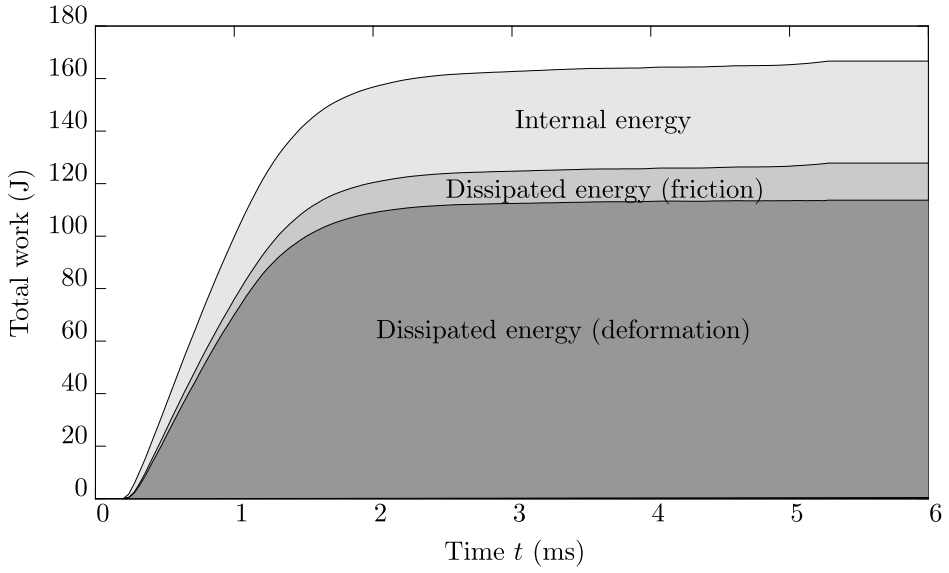

Figure 8: Partition of the total work developed by external forces during a Charpy impact test. The fraction of the total work that has been converted to kinetic energy is negligible, hence not visible.

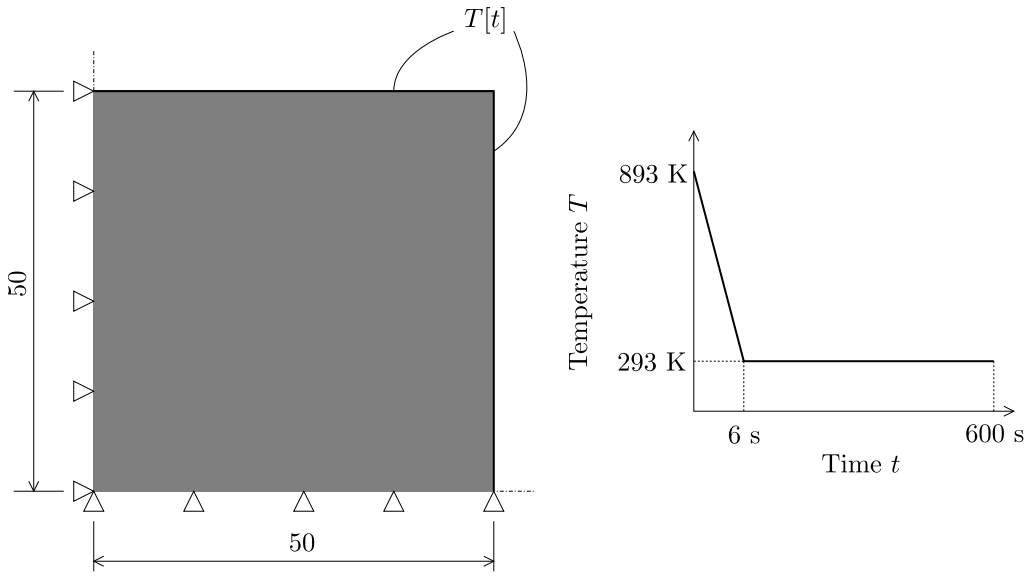

Figure 9: Geometry of the cylindrical specimen and boundary conditions for the simulation of a quenching operation.

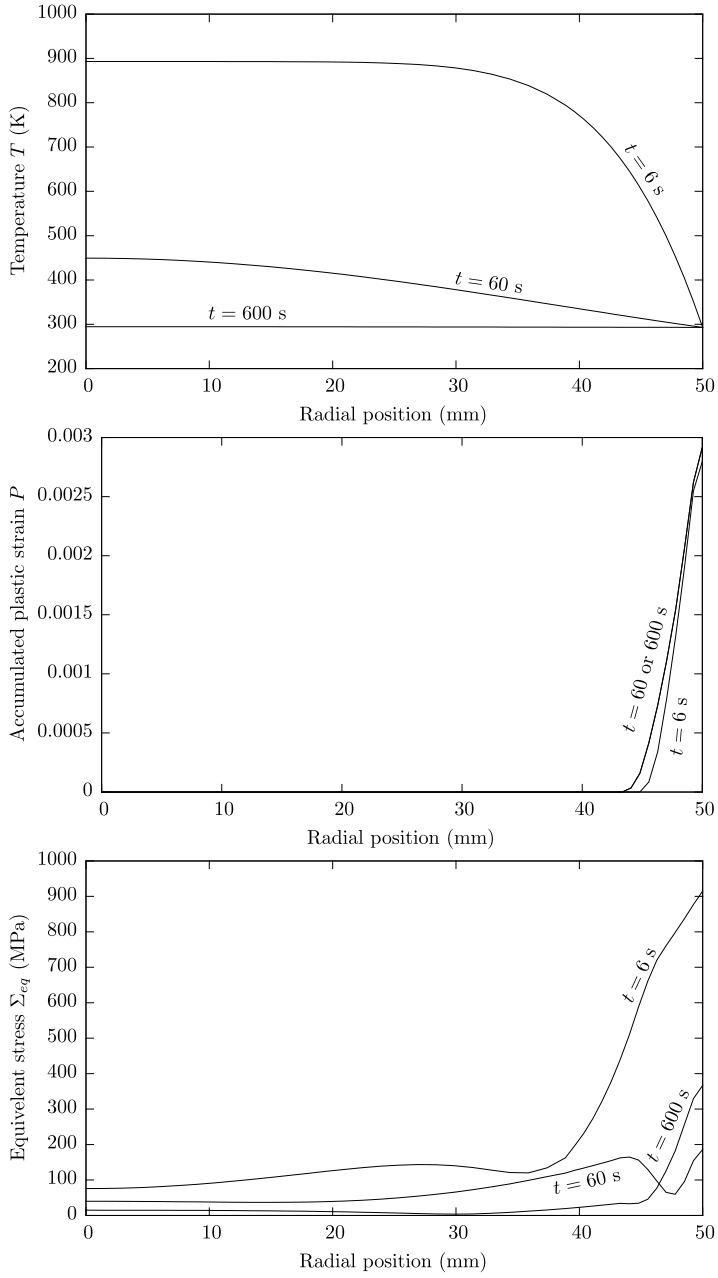

Figure 10: Distribution of the temperature (top), accumulated plastic strain (middle) and equivalent stress (bottom) along a radial path from the center to the external surface of the cylindrical specimen. The time $t = 6$ s corresponds to the end of the cooling stage while the end of the holding stage is at $t = 600$ s.